

# Killing Three Birds with one Gaussian Process: Analyzing Attack Vectors on Classification

Kathrin Grosse  
CISPA, Saarland University  
Saarland Informatics Campus  
kathrin.grosse@cispa.saarland

Michael Thomas Smith  
University of Sheffield  
m.t.smith@sheffield.ac.uk

Michael Backes  
CISPA, Saarland University  
Saarland Informatics Campus  
backes@cispa.saarland

**Abstract**—The wide usage of Machine Learning (ML) has led to research on the attack vectors and vulnerability of these systems. The defenses in this area are however still an open problem, and often lead to an arms race.

We define a naive, secure classifier at test time and show that a Gaussian Process (GP) is an instance of this classifier given two assumptions: one concerns the distances in the training data, the other rejection at test time. Using these assumptions, we are able to show that a classifier is either secure, or generalizes and thus learns.

Our analysis also points towards another factor influencing robustness, the curvature of the classifier. This connection is not unknown for linear models, but GP offer an ideal framework to study this relationship for nonlinear classifiers. We evaluate on five security and two computer vision datasets applying test and training time attacks and membership inference. We show that we only change which attacks are needed to succeed, instead of alleviating the threat. Only for membership inference, there is a setting in which attacks are unsuccessful ( $< 10\%$  increase in accuracy over random guess)<sup>1</sup>.

Given these results, we define a classification scheme based on voting, ParGP. This allows us to decide how many points vote and how large the agreement on a class has to be. This ensures a classification output only in cases when there is evidence for a decision, where evidence is parametrized. We evaluate this scheme and obtain promising results.

## 1. Introduction

The ubiquitous usage of Machine Learning (ML) has opened a whole range of new attack vectors. One targets classifiers at test time, for example Malware detectors [48], [16], speech recognition systems [13], classification for autonomous driving [17], [46], and robot visual systems [32]. Most defenses that are introduced are shown to lead to an arms race [12], [3] in the context of test time attacks. Another attacker affects the model at training time, also called poisoning [31], [7], for example on face recognition systems [6]. In a yet different setting, the attacker

tries to determine whether a particular sample was used in training [56], [24]. This kind of attack is referred to as membership inference.

We tackle the arms race by defining a naive classifier that is secure at test time. When applying a strong assumption to the data and enable rejection, a Gaussian Processes (GP) is an instance of this classifier. Then, however, the covariance matrix of the resulting GP is the identity matrix. This does not allow us to learn [33]. In addition, we observe learning and vulnerability to be influenced by the curvature of the GP. A relationship between vulnerability and curvature is known for linear models like support vector machines [41], and used for mitigations in nonlinear classifiers as well [25], [23]. We investigate this relationship empirically for adversarial examples, poisoning and membership inference.

Finally, we target the threats of test and training time attacks by proposing a new parametrized (ParGP) classification scheme. It sits on top of GP and allows the user to specify how many training points support classification at a given test point. We thereby determine in numbers how well the data supports a classification output. The scheme allows us to defend poisoning by requiring a large support for a decision. For test time attacks, we require that a large number of points agrees on the class. We evaluate this scheme in practice and observe promising results.

Summarized, our contributions are as follows:

- We show that GP is an instance of a naive secure classifier. We prove that this secure classifier is opposed to learning as in generalization. We further conclude that curvature is a factor influencing vulnerability in GP.
- As GPs offer an ideal framework to study curvature of the classification function, we study test, training and membership inference attacks in relation to curvature. To this end, we use five security and two computer vision datasets. Our findings differ greatly among the settings. In test time attacks, we conclude that curvature only changes the kind of attack needed to succeed. In poisoning, we observe only small effects on vulnerability given a predefined curvature. For membership inference, a short lengthscale enables attacks. The maximal increase (if at all) for a

<sup>1</sup>. Please contact the first author to get access to the code used to generate all results in this paper.

TABLE 1. NOTATION USED THROUGHOUT THE PAPER.

| Notation      | Meaning                                                  |
|---------------|----------------------------------------------------------|
| $x$           | data point, equivalent notations: $x_a, X_i$             |
| $y$           | label, equivalent notations: $y_i, Y_i$                  |
| $k(X_i, X_j)$ | covariance function, $K$ corresponding resulting matrix  |
| $\rho$        | a particular value of $k$ (threshold), robustness radius |
| $\kappa$      | some value of $k$                                        |
| $B(x, \rho)$  | ball around $x$ with radius $\rho$ , also $\rho$ -ball   |
| $\mu$         | GP prediction                                            |
| $p$           | some value of $\mu$                                      |
| $\delta$      | malicious perturbation for data point                    |
| $\epsilon$    | parameter to globally perturb data point                 |
| $l$           | lengthscale of GPs covariance (RBF)                      |

long lengthscale is  $< 10\%$  attack accuracy compared to random guess accuracy.

- We finally propose as a solution to the vulnerability towards test and training time attacks. We introduce and evaluate ParGP, a parametrized classification scheme based on GP.

## 2. Background

In this section we present the necessary background for this work. We start by introducing classification and GP, give a short summary of adversarial learning and finally summarize our threat model.

We are mainly concerned with classification: In classification, the task is to assign labels  $Y$  to some data samples  $X$ . In general, we separate the data into training ( $X_{\text{tr}}, Y_{\text{tr}}$ ) and test data ( $X_{\text{t}}, Y_{\text{t}}$ ). We then adapt the parameters of a classifier function  $f$  such that  $f(X_{\text{t}}) = Y_{\text{t}}$  for the unseen test data. We summarize the notation used in this paper in Table 1.

### 2.1. Gaussian Process Classification

We introduce Gaussian Process Classification (GPC) [39] for two classes using the Laplace approximation. The goal is to predict the labels  $Y_{\text{t}}$  for the test data points  $X_{\text{t}}$  accurately. In GP, we use a covariance function, which can be seen as a kernel or similarity metric in ML. We will use those names interchangeably in this paper.

We first consider Gaussian Process regression (GPR), and assume that the data is produced by a GP and can be represented using a covariance function  $k$ :

$$\begin{bmatrix} y_{\text{tr}} \\ y_{\text{t}} \end{bmatrix} = \mathcal{N} \left( 0, \begin{bmatrix} K_{\text{tr}} & K_{\text{tt}} \\ K_{\text{tr}}^T & K_{\text{t}} \end{bmatrix} \right), \quad (1)$$

where  $K_{\text{tr}}$  is the covariance of the training data,  $K_{\text{t}}$  of the test data, and  $K_{\text{tt}}$  between test and training data. Having represented the data, we now review how to use this representation for predictions. As we use a Gaussian model, our predictions are Gaussian too, with a predictive mean and a predictive variance which we define now. At a given test point  $x$ , assuming a Gaussian likelihood function, the predictive mean is

$$y_{\text{t}}^* = K_x^T K_{\text{tr}}^{-1} y_{\text{tr}}, \quad (2)$$

where  $K_x^T$  is the vector with the distances from  $x$  to each training point. Analogously, we can compute the predictive variance of for the test data as

$$\text{var}(y_{\text{t}}^*) = K_{\text{t}} - K_{\text{tr}}^T K_{\text{tr}}^{-1} K_{\text{tt}}. \quad (3)$$

We will not detail the procedure for optimizing the parameters of the covariance function  $k$  that defines our Gaussian prediction. Instead, we outline how to alter this regression model to perform classification. Since our labels  $y_{\text{t}}$  are not real valued, but class labels, we rewrite Equation (2) as

$$y_{\text{t}}^{**} = \sigma(K_x^T K_{\text{tr}}^{-1} y_{\text{tr}}), \quad (4)$$

where we apply a link function  $\sigma(\cdot)$  that normalizes the output to be in range  $[0, 1]$ . This procedure is called Laplace approximation.

In the formal analysis, we focus on regression: it is similar to the latent representation that is used for the prediction in Laplace approximated classification (GPC). More concretely, when the mean of regression goes towards one class, GPCs classification will do so as well. As we are not interested in the strength of a response in our analysis, we thus skip the additional steps introduced by  $\sigma(\cdot)$ . Finally, whenever we write GP, we refer to properties that both GPC and GPR share.

**2.1.1. Covariance Function.** We introduce the most common similarity metric in GP, the RBF kernel. This metric is defined as follows

$$k(x_i, x_j) = \exp \left( - \frac{l|x_i - x_j|_2^2}{2\sigma^2} \right), \quad (5)$$

where the  $L_2$  distance between two points is rescaled by lengthscale  $l$  and variance  $\sigma^2$ . As we use the exponential function, the output similarity approaches 0 as the distance gets larger. This property is called abatement, and useful for outlier detection or open set tasks [42]. We can influence how fast the kernel decays by setting lengthscale  $l$ .

### 2.2. Adversarial Machine Learning

Given a trained classifier  $f(\cdot, \theta)$ , test-time attacks compute a small perturbation  $\delta$  for a test sample  $x \in X_{\text{t}}$  such that

$$\min \delta : f(x, \theta) \neq f(x + \delta, \theta). \quad (6)$$

In a nutshell, we try to find a minimal perturbation  $\delta$  given some metric that changes classification. Using Equation (2), we rewrite the equation for GP as

$$\min \delta : \max \zeta : |K_x^T K_{\text{tr}}^{-1} y_{\text{tr}} - K_{x+\delta}^T K_{\text{tr}}^{-1} y_{\text{tr}}| = \zeta, \quad (7)$$

where  $K_{x+\delta}$  denotes the new distances for a point with added perturbation  $\delta$ . We introduced an additional parameter,  $\zeta$ , denoting the change in output space for perturbation  $\delta$ , e.g. the change leading to a different classification output.

Many algorithms to compute  $\delta$  have been introduced on Deep Neural Networks [52], [37], [11], but also on other algorithms [5]. Defending models is still an open task [12]

although a multitude of defenses have been proposed, among them game theory [10] and robust optimization [30].

The range of attacks is however not only limited to test-time attacks, but also training data can be maliciously altered (poisoned). The goals of poisoning vary: sometimes the parameter vector  $\theta$  of the classifier is manipulated [31]. Other goals include the changing the classification for individual points, areas of the feature space or entire classes [7], [34]. When we are interested in the misclassification of a single test point, we can formalize this for GP as

$$\min \delta : \max \zeta : |K_x^T K_{tr}^{-1} y_{tr} - K_{x \oplus \delta}^T K_{tr+\delta}^{-1} y_{tr}| = \zeta, \quad (8)$$

where we write  $K_{tr+\delta}^{-1}$  for the new distances of the modified training data. We further write  $K_{x \oplus \delta}^T$  for the changed distances of the training data to  $x$ . Here we simplify strongly by writing the effect of optimization or training as  $tr + \delta$  and  $x \oplus \delta$ , to show the relationship by the inverse function theorem. Analogous to test time attacks, a range of defenses has been proposed for poisoning [26], [15], [50].

Another area of adversarial learning includes Model stealing as investigated by Tramer et al. [44]. Membership inference, e.g. the question whether a training point was used or not, has been tackled by Shokri et al. [56] for discriminative models and for generative models by Hayes et al. [24].

Another, orthogonal line of work includes bugs [51] and byzantine failures [8] in ML. These are not dealt with in this analysis, as they often concern parallelization or the code of the ML system.

### 2.3. Threat Model

In this paper, we consider three different attackers. One targets the model at training time, to change classification for a single test point. The other two attack at test time, albeit with different goals. One tries to mislead the model when it computes a prediction. The last one tries to infer from a trained model whether a particular data point was used in training or not.

Concerning knowledge about the model, any of these attackers might have full knowledge of the model (white-box), where she can access each parameter of the trained algorithm. The grey-box setting considers information about the algorithm applied, where the parameters are however unknown. In the black-box model, the attacker has no knowledge about the model, not even which algorithm is used.

Analogously, we have to take into account the knowledge the attacker has about the data. The training data might be fully known. If access is restricted, the attacker might have learned the kind and/or the number of features. In a more difficult setting, nothing except the task is known.

The capabilities of our three attackers vary between the settings. The test time attacker that tries to fool the model knows the feature space and task, has however no knowledge about the model. The training time attacker has as well knowledge about feature space and task, and is given

full access to the model to compute the gradients. The last attacker, performing membership inference, is the strongest one with full knowledge about training and test data. We assume this knowledge in an effort to study a worst-case attacker.

## 3. A Secure classifier at Test Time

In this section, we define a naive secure classifier, show its relation to other classifiers and evaluate its performance on several datasets.

### 3.1. Formal Definition

The secure classifier assumes correctly labeled training data. We further assume a similarity metric for which we know a radius around each training point such that the associated class does not change. By classifying inside this radius and rejecting otherwise, the classifier is secure by definition.

We use an abating similarity measure: as the distance from the training data increases, the measure approaches 0. There is a  $\rho$  such that for all training points, iff point  $x'$  is in  $B(x, \rho)$ , or the closed ball around  $x$  with radius  $\rho$ , then  $x'$  cannot be an example of another class than  $x$ . In other words, all points in the  $\rho$ -ball around  $x$  are of the same class. We formalize secure classification as

$$f(x') = \begin{cases} y_i & \text{iff } x' \in B(x_i, \rho) \\ \text{reject} & \text{otherwise} \end{cases}$$

and obtain a secure classifier which cannot be fooled. Changing a sample enough to be classified as a different class means to alter  $x'$  so much that  $x' \in B(x_j, \rho)$  where  $i \neq j$ . Then, however,  $x'$  is a valid instance of this class.

We now briefly the relationship of the secure classifier to other classifiers. The constant classifier, which is also secure, is then a special instance of the classifier described here, where the number of points is one and  $\rho = \infty$ . The secure classifier is further equivalent to a 1-nearest-neighbor classifier using a threshold  $\rho$ .

### 3.2. Evaluation of the Secure Classifier

The theoretical existence of a secure classifier raises the question of its usefulness in practice. We thus evaluate the classifier introduced in Equation (9). First, we describe all datasets (Table 2 gives an overview) used for evaluation. We then detail our evaluation procedure and present our results.

**3.2.1. Data.** We evaluate the classifier on a range of tasks, focusing on security settings such as Malware/Spam detection. We however also introduce other loosely security related tasks, such as credit card applications, fake banknote detection, and computer vision.

TABLE 2. OVERVIEW OF DATASETS USED.

| Name      | # Features | # Instances | Random Guess Accuracy | Features |
|-----------|------------|-------------|-----------------------|----------|
| Hidost    | 1, 223     | 439, 563    | 96%                   | mixed    |
| DREBIN    | 545, 333   | 129, 013    | 90%                   | binary   |
| Spam      | 54         | 4, 601      | 70%                   | mixed    |
| Credit    | 14         | 690         | 60%                   | mixed    |
| Bank      | 4          | 1, 372      | 51%                   | real     |
| MNIST     | 784        | 70, 000     | 10% / 50%             | real     |
| SVHN      | 3, 072     | 99, 289     | depends on task       | real     |
| two moons | 2          | 100         | 50%                   | real     |

**Hidost.** The first Malware dataset consists of the PDF Malware data of the Hidost Toolset project [49]. We use the 439,563 PDF Malware samples, of which 32,567 are malicious and 407,037 are benign. Each sample consists of 1,223 features, where feature vectors are likely to be sparse. We use 95% of the data for training and 5% for testing.

**DREBIN.** The second, an Android malware dataset (introduced by Arp et al. [2]) contains 123,453 benign and 5,560 malicious Android Applications, totaling 129,013 instances. Each sample consists of 545,333 binary malware features. As the number of features in this dataset is very large, we restrict ourselves to the manifest features (as was done in previous work on adversarial learning on this dataset [21]). This leaves us with 233,655 binary sparse features. The dataset

**Spam.** The third dataset contains 4,601 samples for Spam detection [28]. The number of features is 57 of which 54 features are continuous and represent word frequencies or character frequencies. The three remaining integer features contain capital run length information. This dataset is slightly imbalanced: roughly 40% of the samples are classified as Spam, the remainder as benign emails. We split this dataset randomly and use 30% as test data.

**Credit.** The fourth dataset contains 14 features about Australian credit card applications and whether or not they were granted [28]. The features are real, binary, and nominal. There are 690 instances, or applications, 44.5 of which were granted. We split this dataset randomly and use 30% as test data.

**Bank.** The fifth dataset contains 4 precomputed features from pictures of banknotes [28]. For each of the 1,372 instances, we must decide whether the banknotes are real or fake. All features are real valued, with both classes being the same size. We split this dataset randomly and use 30% as test data.

**MNIST.** The sixth dataset we use is the MNIST benchmark dataset [27]. It consists of  $28 \times 28$  pixel black and white images of handwritten single digits. There are 50,000 training and 10,000 test samples, with all classes roughly the same size. From this dataset, we select a variety of number vs. number and number vs. all others tasks.

**SVHN.** Finally, we use the SVHN dataset [36]. It consists of  $32 \times 32$  colored images of house number digits. There are 73,257 training and 26,032 test samples. Analogously to the MNIST dataset, we pick several different subtasks.

**3.2.2. Setting.** We use several similarity metrics to evaluate the secure classifier. We use the RBF kernel from Section 2.1.1, the Laplace kernel, the Chi-Square kernel, and SSIM, a perceptual distance metric [54].

We take a simple approach to approximate the threshold  $\rho$ . We determine the highest similarity  $s_{max}$  observed between two points of opposing classes. Then, we define the threshold  $\rho = s_{max}/2.0$ .

We measure the accuracy given this classification scheme. As a baseline, we report the accuracy without a threshold (output is then the class of the nearest neighbor, or 1-nearest-neighbor classifier). Except SSIM<sup>2</sup>, all of these distances are parametrized. We thus test accuracy and threshold for a range of parameters, namely from  $e^{-5}$ ,  $e^{-4}$ , ... to  $e^{+5}$ .

**3.2.3. Results.** We plot the results on several datasets in Figure 1. We omit MMNIST, Bank and Malware task as the accuracy of (1NN) is always  $> 98\%$  and the accuracy of the secure classifier close to zero. The only exception is SSIM, which generally leads to random guess accuracy using the threshold. We conclude that the distance between the closest samples of opposite class is much closer than the distance between benign training and test data.

Analogously to [53], we evaluate how to improve security by deleting points from the training set to improve the threshold. In particular, we delete the points that are closest to the opposite class to obtain a larger threshold. Using this method, we do not observe an increase in accuracy. We conclude that the threshold does not increase fast enough to make up for the deleted points needed for classification.

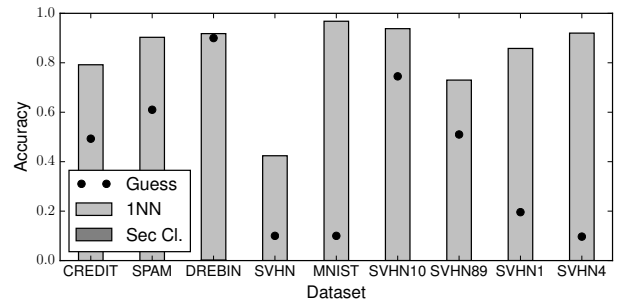


Figure 1. Accuracy of Secure classifier (dark grey, always close to zero) and 1-nearest-neighbor (1NN, gray) compared to random guess (black dot).

## 4. GP and Secure Classifier

In this section, we show that GP can be an instance of the secure classifier as described in the previous section. This equivalence allows us to show that learning is opposed to static security guarantees. We further derive factors that influence vulnerability in GP.

2. SSIM can be parametrized, however the originally proposed version corresponds to a value of 1.5 as parameter which is used here.

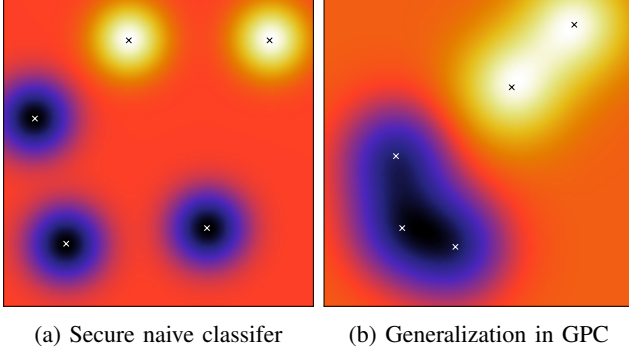


Figure 2. Secure classifier and generalization in GPC. Black and white points are training data. The axis are the two features.

In the previous section, we introduced a naive secure classifier. As we show now, GPR is equivalent to this secure classifier, given the following assumptions:

- 1) GP rejects has a rejection option based on  $\rho$ ,
- 2) There is no point  $x'$  such that for two distinct  $x_i, x_j \in X_{tr}$  both  $k(x_i, x') > 0$  and  $k(x_j, x') > 0$ ,

where assumption two states that the similarity between any two training points is zero, independent of the class. Given the last assumption holds, however, the resulting covariance matrix is the identity matrix, as the similarity between any two points is zero. This matrix does not allow any learning [33].

We implicitly assume here that these assumptions hold as well for the secure classifier. If they do not, we enforce them by deleting training data, for example. We also implicitly assume that  $\rho$  is equivalent for all training points. In case of different  $\rho$ s, we apply the smallest. Further, in the infinite sample limit, the secure classifier might cover the whole generating distribution of the data. It is then again equivalent to a GP as well, given the data distribution is a Gaussian distribution itself. For security in the infinite sample limit in general, refer to [53]. Our analysis concerns a set of finite samples.

We start by showing that given the previous two assumptions, GP is indeed equivalent to the classifier presented in Equation (9).

#### 4.1. GP as a Secure Classifier

We visualize the classifier derived here given the assumptions in Figure 2a. The predictive mean of GPR is composed of weighted labels, where the weight is related to the similarities between the training points and the distance to the queried test point Equation (2).

When assumption two holds, the kernel matrix is the identity matrix: the similarity between any two points is zero, and the similarity of each point with itself is 1.0. A test point  $x'$  is at most close to a single training point, here  $x_n$ . We summarize:

$$\mu' = k(x', x_n) * 1 * y_n, \quad (10)$$

where 1 denotes the similarity from  $x_n$  to itself; all other terms are zero as  $k(x', x_i) = 0$  iff  $i \neq n$ . This classifier is almost equivalent to Equation (9), as it classifies each point if it is in the  $\rho$ -ball of any training point.

To fulfill assumption one, we define rejection for GPR. We need to reject any test point for which  $k(x', x_n) \leq \rho$ . As the minimum and maximum output of GPR as reasoned above are either 1 or  $-1$ , we do not classify a sample iff

$$\mu \in [-1 + \tau_0, 1 - \tau_1], \quad (11)$$

where we chose  $\tau_0 = \tau_1 = \rho$  to reject points further away than  $\rho$ . We can actually define a different thresholds for the two classes if required.

#### 4.2. Generalization and Secure Classifier

Let us assume the second assumption does not hold. As the similarity between some points is not 0 anymore, they will jointly influence classification as visualized in Figure 2b. This is called generalization.

**Theorem 1.** *Learning in GPR involves classifying areas outside the  $\rho$ -balls (generalization), or there is no improvement over GPR with rejection and an identity matrix as covariance.*

**Proof.** To be classified, we need an output  $> \rho$  or  $< -\rho$ . We start with the first case. We thus obtain prediction

$$p \leq \sum_i (\rho - \kappa_i) * K_i^{-1} * 1, \quad (12)$$

where  $K_i^{-1}$  is the sum over the inverted covariance matrix column corresponding to point  $i$ . Before inversion, this column contains the similarities between  $i$  and all other training points.

So far, we have ignored that we actually need a test point to obtain this prediction. Without loss of generality, we pick  $x'$  which maximizes the above sum under the restriction that  $x'$  is in none of the  $\rho$ -balls (hence  $\rho - \kappa_i$ ). There are three cases. In the first,  $p \geq \rho$  and we classify outside the  $\rho$ -ball.

In the second case,  $p = 0$  or  $0 < p < \rho$ . As we reasoned about the maximal  $x'$ , we know that there are no other points for which  $p > \rho$ . Then GPR is still secure: no area outside the  $\rho$ -ball is classified, as the output is below the defined threshold. It remains to be shown, however, that there is no contradiction for the opposite class. We proceed analogously with an  $x$  that is chosen to minimize the sum. ■

**Remark.** We used in the proof that the minimal output of a point chosen to maximize the sum is zero. Analogously, the maximal value when minimizing the sum is zero as well. This holds due to the abating property of the kernel: As we move away from the data, eventually all distances become zero, thus the sum is zero as well.

We conclude that generalization leads to classification in areas which might enable test time attacks such as adversarial examples. Before we address adversarial examples, however, we address the rejection option in GP once more.

### 4.3. Rejection in GP

Let us assume once again that our covariance matrix is the identity matrix, and the covariance metric RBF. For two points  $x_i$  and  $x'$ , where  $|x_i - x'|_2^2 = d$ , we observe that

$$\tau_i = \rho = \exp(ld/2\sigma^2) * 1 * 1, \quad (13)$$

can be solved for either  $l$  or  $\sigma^2$  when fixing the other term. We further affect  $\rho$  by adapting  $l$ . This means that by changing  $l$ , we change the radius of the ball each point is classified in.

Yet, this reasoning holds only when the covariance is identical to the identity matrix. In other cases, as the distances are nonzero, they also affect the sum  $K_i^{-1}$ . Hence, the terms in the inverse covariance matrix do necessarily not add up to one anymore. The threshold is then defined over a distribution and loses its interpretation as a radius around an individual point.

At the same time,  $l$  determines the gradient of the GP. For fixed training data, we observe that the gradient of the kernel for a given fixed point  $x^*$  is

$$\frac{\partial k(x^*, x)}{\partial x_i^*} = \sigma^2 \frac{1}{l^2} (x_i - x_i^*) k(x^*, x) \quad (14)$$

depending on the distance to other (training) data points  $x$ , the lengthscale  $l$  and variance  $\sigma^2$ . As  $l \rightarrow 0$ , the gradient goes to infinity: We conclude that GP's prediction surface can be arbitrarily steep, to fit classes for confident classification even if those classes are arbitrarily close. At the same time, as  $l \rightarrow \infty$ , the gradient goes towards 0.

The choice of this lengthscale parameter,  $l$ , relates to regularization in the framework of GP [41]. As for linear methods, we can thus conclude that there is a relationship between robustness and regularization.

In contrast to regularization in linear methods, however, we can fix a lengthscale for GP before training. The second case, where the lengthscale is optimized and learned during training, is not considered here. Instead, we are able to directly investigate the effect of curvature on empirical vulnerability. We address this relationship in the next sections.

## 5. GP and Test Time Attacks

In the previous section, we showed that generalization or learning leads to classification outside the  $\rho$ -balls. We might by generalization however also misclassify inside a  $\rho$ -ball. One case is when the two balls intersect (Figure 3, left plot). In a more complicated setting, several points of opposite class vote stronger than a single point, shifting the classification boundary inside the  $\rho$ -ball (Figure 3, right plot).

On the other hand, there are settings where the attacker is not limited to a small change to a sample, for example in Malware detection: in contrast to images, changes are harder to perceive for humans. To tackle very unusual samples (possibly caused by large changes), we study the effect of abatement and rejection in classification. These effects combine to a build-in outlier detection in our model.

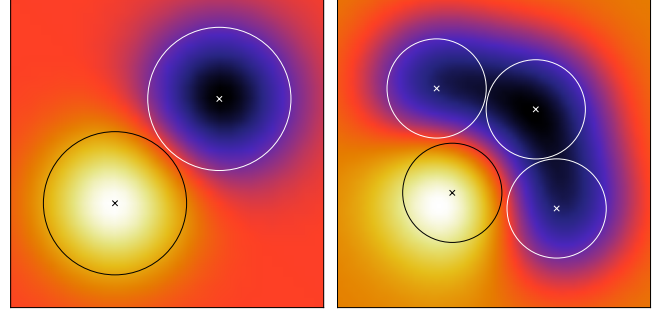


Figure 3. Generalization in GPC. Bright and Dark areas are classes, other areas (red) rejection areas. Black and white points are training data, circles  $\rho$ -balls. The axes are the two features.

TABLE 3. WE DEPICT THE NUMBER OF SAMPLES USED FOR TRAINING, THE CHOSEN LENGTHSCALES AND ACCURACIES WITH REJECTION OPTION (IF  $\mu = 0$ , ACCURACIES WITHOUT REJECTION ARE IN FIGURE 4). FINALLY WE REPORT THE  $\delta$  PICKED FOR POISONING.

| Dataset | # samples | short $l$ |      | long $l$ |      | Poison     |            |
|---------|-----------|-----------|------|----------|------|------------|------------|
|         |           | $l$       | Acc. | $l$      | Acc. | $\delta_l$ | $\delta_h$ |
| Hidost  | 500       | .5        | 98.4 | 1.9      | 97.7 | .4         | 1.0        |
| Drebin  | 750       | .5        | 54.4 | 1.9      | 94.8 | .4         | 1.0        |
| Spam    | 500       | .3        | 92.6 | 5        | 92.7 | .15        | 2.2        |
| Credit  | 500       | .3        | 89.4 | 2        | 87.9 | .15        | .75        |
| Bank    | 500       | .3        | 100  | 2        | 100  | .15        | .75        |
| MNIST91 | 500       | 1         | 98.9 | 8        | 99.5 | .75        | 2.5        |
| MNIST38 | 500       | 1         | 93.4 | 8        | 97.4 | .75        | 2.5        |
| SVHN91  | 1500      | 8         | 85.4 | 16       | 83.8 | 6          | 12         |
| SVHN10  | 1500      | 8         | 88.7 | 16       | 88.7 | 6          | 12         |

### 5.1. Setting

**Data and Methods.** We use the same datasets as in the previous experiments, which we summarized in Table 2. Additionally, we employ the two moons dataset in two dimensions for visualization. We further train a GP with a predefined lengthscale and observe accuracy with and without rejection and on malicious data.

**Implementation.** We implement our experiments in Python using GPy for the Gaussian Process approaches [20]. We show further information on the trained GPCs in Table 3, such as the number of training samples used. To obtain adversarial examples, we use Tensorflow [1], the Cleverhans library 1.0.0 [19], and public implementations for all other attacks [11], [22].

### 5.2. Lengthscale and Rejection Option

The lengthscale allows us to specify how fast the similarity decays. This influences how far we can shift a point before it is rejected. Conversely, if the metric abates too fast, the classifier cannot capture the variance between test and training data and generalizes poorly. To evaluate the effect of  $l$ , we train GPCs using different lengthscales on all datasets. We monitor accuracy and compute the AUC, both on test data. AUC is the area under the ROC (Receiver Operator



Curve). This curve shows on the y-axis the accuracy of the classifier given some parameter (here the threshold). As this is not a binary task anymore (third *class* is rejection), the AUC can be smaller than 0.5. In this experiment, we use only benign data. The more area below the curve, the better. For GP, if the area is large, the data is confidently classified with a large difference in output for the classes. No test data lies in areas of low certainty, and we can confidently reject data there.

We depict the results in Figure 4. We observe for all datasets that there is a range where accuracy is high and AUC is very small. In these areas, GPC classifies correctly, but is not very confident on the test data. In many cases, we observe that the interval is large when accuracy decreases: there are distinct lengthscale values for a confident rejection and high accuracy. We conclude that good accuracy and confident classification (and thus good rejection) are not necessarily linked.

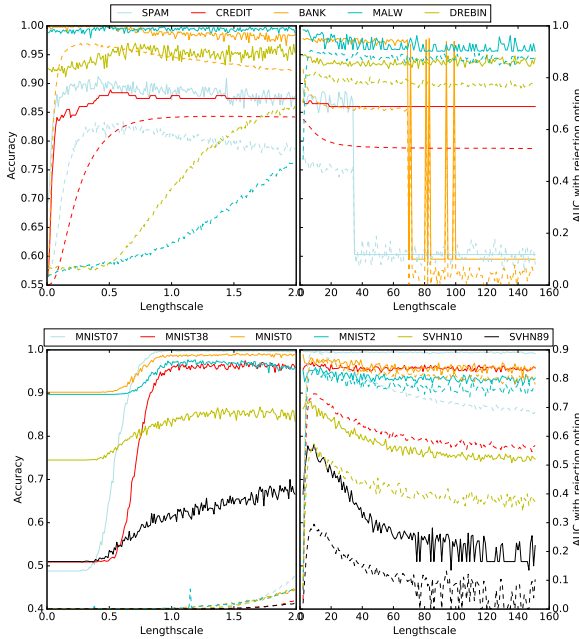


Figure 4. Relationship between Rejection Option, Accuracy and lengthscale for GPC and RBF kernel on different tasks. We plot Accuracy (lines) and AUC (dotted lines).

### 5.3. Lengthscale and Vulnerability

Given only the gradient of the kernel, we expect that a GPC with a long lengthscale misclassifies fewer adversarial examples. We have crafted adversarial examples on several of our datasets (Spam, Bank, Credit, HiDost, MNIST91, MNIST38, SVHN91, SVHN10) on a range of algorithms (DNN, GPC, linear SVM) and compare the vulnerability of two GPCs, one with a long and the other with a small lengthscale. We sort the attacks according to  $\epsilon$  for global perturbation. We summarize all attacks based on the Jaco-

bian in JBM, and plot all attacks by Carlini and Wagner according to the norm optimized ( $L_x$ ) for norm  $x$ .

We further chose the lengthscales according to the previous experiments, where both achieve similar accuracy on benign data (for example, 0.5 and 2.0 for Spam or 8.0 and 16.0 for SVHN91). The results are depicted in Figure 5, where we only distinguish different datasets. We observe that correct classification is on average higher when the lengthscale is shorter. In particular, we observe attacks with global perturbation ( $\epsilon > 0.01$ ), a shorter lengthscale performs better. For highly optimized attacks ( $L_2$ ), a longer lengthscale is of advantage.

We additionally allow for a rejection option, as we previously forced GP to output a classification. Instead, we now reject if  $\mu = 0$ : in this case, the test point is far away from the training data. A short lengthscale might thus allow us to more easily reject abnormal data. As we observe in Figure 6, adding a rejection option when using a long lengthscale has no effect at all. For a short lengthscale, the effect is positive or neutral, and only negative two cases. These two cases stem from the Hidost dataset, which is highly imbalanced, and the assignment of forced classification was in favor of the dominant class.

To understand the effect of lengthscale on modified data, we investigate a toy example. We depict GPC with two different lengthscales on the two moons dataset in Figure 7. We observe that using a long lengthscale, the density mass is pushed away from the training data, and the classifier is confident in areas where there is no training data. The results on the individual attacks confirm this: highly optimized attacks such as Carlini and Wagner and some cases of Jacobian attacks are more often classified correctly with a long lengthscale (boundary areas), whereas for non targeted attacks ( $\epsilon$ ) a shorter lengthscale is beneficial.

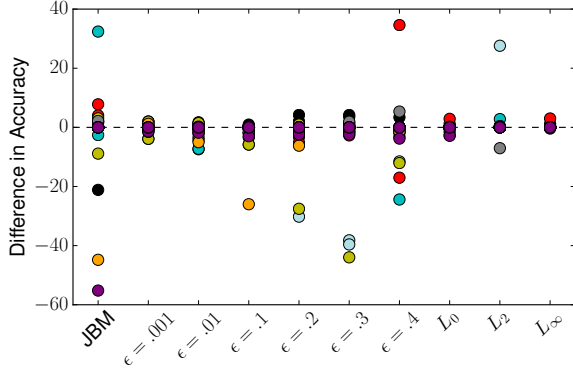
### 5.4. Conclusion on GP and Test time Attacks

Our first observation is that a good accuracy does not imply confident classification. We further conclude that robustness is related to the lengthscale in practice, as argued in the previous section. A long lengthscale is more robust towards optimized attacks, such as  $L_x$ -attacks methods based on Jacobian. In contrast, a short lengthscale rejects more examples that are not targeted, like fast gradient approaches. In general, we observe rejection to increase robustness only for a short lengthscale. As GPC is an example of a nonlinear method, our analysis implies the necessity to evaluate any mitigation or defense on range of *diverse* attacks, not only highly optimized ones.

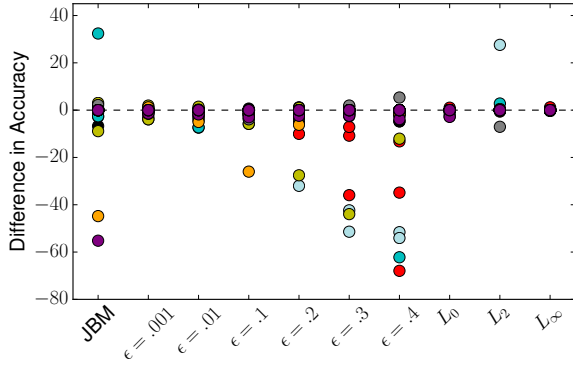
## 6. GP and Poisoning

We will now turn to another attack vector: we investigate the effect of the lengthscale on training time attacks on GP.

For the naive secure classifier, poisoning is straight forward. If we introduce a point  $x_p$ , everything in its  $\rho$ -ball will be classified as  $y_p$ . Usually, the training procedure has to be taken into account to ensure efficient poisoning



(a) Forced Classification.



(b) With Rejection Option.

Figure 5. Vulnerability and Lengthscale Size in GPC. Above zero denotes that more examples are correctly classified (or rejected) by a GPC with a long lengthscale. Below zero more example are correctly classified or rejected when using a short lengthscale.

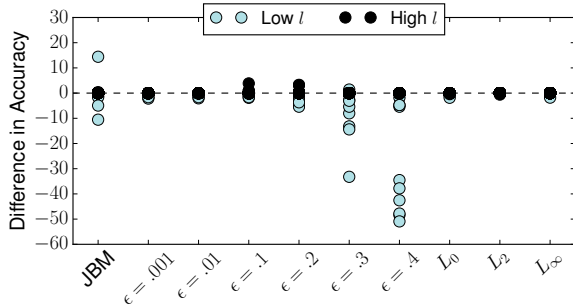


Figure 6. Vulnerability, Lengthscale and rejection option in GPC. Above zero denotes that more examples are correctly classified or rejected by a GPC without a rejection option. Datasets as in Figure 5.

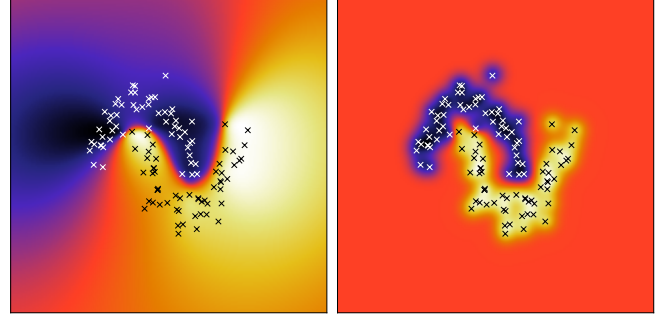


Figure 7. Lengthscale and extrapolation of GPC on the two moons dataset. Left figure uses a lengthscale which is 12 times the lengthscale of the right graph to emphasize the effect.

attacks. In GP, the poisoned training data will yield different parameters for  $k(\cdot, \cdot)$ . Adding one point affects further all other points in  $K_i^{-1}$  (by one term for each added point). A formal bound on the change in output that a manipulated label introduces in GPC (in the context of privacy) has been investigated in [47].

Here, however, we fix the lengthscale of GP, which minimizes the effect of the training or optimization on the kernel function  $k$ . The covariance matrix will however still be changed, and also GP still optimizes the covariance function to separate the data well. In other words, we investigate in this section how much a classifier changes when training on manipulated training data, given this classifier is computed globally (long lengthscale) or locally (short lengthscale).

Partitioning the prediction for test point  $x$  into both classes as

$$\sum_i (k(x, x_i) K_i^{-1} 1) + \sum_i (k(x, x_i) K_i^{-1} * -1), \quad (15)$$

allows us to approximate how many malicious points we need to introduce. In an area where the mean is zero because all points are far away, adding one point suffices. When there are many points of the opposite class, however, a single point is overruled by its surrounding points. We will empirically investigate how many points have to be introduced for poisoning in this section.

## 6.1. Poisoning Attack for GP

We introduce a gradient based attack, formalized in Algorithm 1. We input a sample  $x$  and  $\delta$ , or the  $L_2$  distance of the poisoning points to  $x$ . We additionally specify how many points are introduced ( $n$ ) and use the classification function  $f_*$  to compute the gradients. We re-weight the gradient by already modified features to increase diversity. Further, we change features only by the difference to the target value ( $1, -1$  for normalized features) to obtain valid data points. Albeit assuming access to the model here, the attack can be combined with model stealing.



**Algorithm 1** GP Poisoning

---

```

1: Input: sample  $\mathbf{x}$ , parameters  $\delta, f_*, n$ 
2:  $\text{XPoison} \leftarrow \{\}$ 
3:  $\text{global\_}\delta \leftarrow \{\}$ 
4: for  $i < n$  do
5:    $\text{local\_}\delta \leftarrow 0$ 
6:    $x_p \leftarrow \mathbf{x}$ 
7:   while  $\text{local\_}\delta < \delta$  do
8:      $\text{grads} \leftarrow \nabla f_*(\mathbf{x})$ 
9:      $x_p, \text{global\_}\delta \leftarrow \text{perturb}(x_p, \text{grads}, \text{global\_}\delta)$ 
10:     $\text{local\_}\delta \leftarrow \|\mathbf{x}_p - \mathbf{x}\|_2^2$ 
11:   end while
12:    $\text{XPoison} \leftarrow \text{XPoison} \cup x_p$ 
13: end for
14: return  $\text{XPoison}$ 

```

---

**6.2. Lengthscale and Poisoning**

**6.2.1. Setting.** We use the same datasets as in the previous experiments in Section 3.2 and Section 4, which we summarized in Table 2. Analogously to before, we implement our experiments in Python using GPy for the Gaussian Process approaches [20]. We use the low and high lengthscale values from previous experiments and train the GPC as depicted in Table 3. In this table we also detail the two  $\delta$  used to compute the attack.

For each dataset, we pick 30 points which are not used for test or training. We try to flip the label as assigned by a GPC trained on benign data. Further, we monitor the change in  $\mu$  for each trained classifier, where we train a separate GPC for each  $n$  poisonous points for each single target. We run four sets of experiments: for both lengthscales  $l_{\text{low}}$  and  $l_{\text{high}}$ , we chose two  $\delta$ , such that  $\delta_l < l_{\text{low}} < \delta_h < l_{\text{high}}$ .

**6.2.2. Results.** We show the results of our experiments in Figure 8. We observe in the last four plots that the size of  $\delta$  has few influence on poisoning. Only two datasets, Spam and Credit, are much harder to poison with larger  $\delta_h$ . We will thus in the following discuss only the results on  $\delta_l$  in the upper graphs.

As expected, we observe that changes are larger when more points are introduced. When one point is added most of the data to be close to the diagonal (the change between initial and final lengthscale is small) for both lengthscales. For a long lengthscale, it is harder to poison points with a high initial confidence: points close to zero and one are shifted less than other points, for example between 0.2 and 0.8. For a short lengthscale, the output for some datasets such as MNIST8 and Hidost is initially around 0.5. On two datasets, Spam and Bank, we observe almost no misclassification.

For some datasets, in particular when the initial confidence was not very high, introducing a single point suffices to cause misclassification. For the majority of points, also more confident ones, 5 points are sufficient.

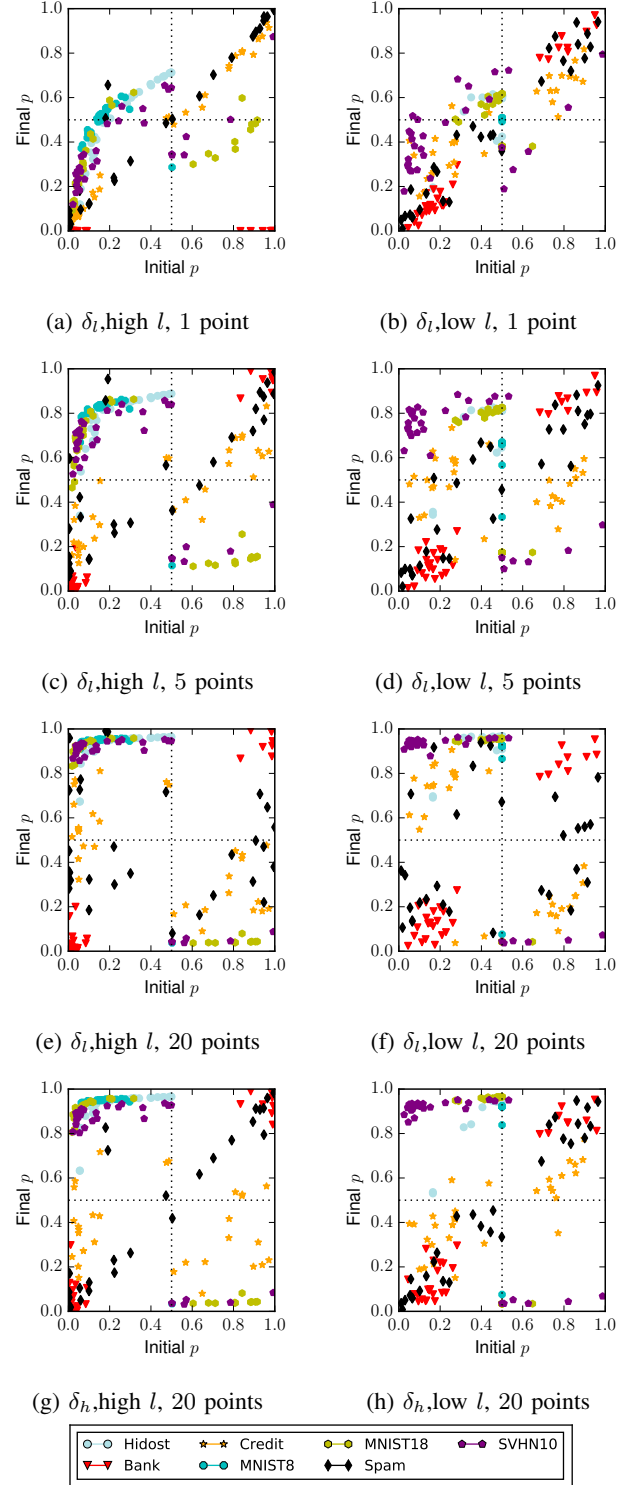


Figure 8. Poisoning in GPC. Each plot shows one  $\delta$ , lengthscale and number of malicious points introduced. Each point in a plot is one target point with its initial and final (after poisoning) confidence. Decision boundary of GP is 0.5 (dotted): right upper and left lower square are correct classification.

### 6.3. Conclusion on GP and Poisoning

We observe that in practice, both lengthscales are vulnerable. For a larger lengthscales, more poisoning points need to be introduced to achieve a strong change in output when the initial classification was confident. Given a short lengthscales, we observe instead that many datasets are classified with low confidence. In general, however, the number of malicious points needed to cause misclassification is small: one to five points suffice.

## 7. GP and Membership Inference

We now turn to membership inference, or the question whether we can infer which training data was used to train the algorithm. We will first discuss formal indications about membership inference, propose an attack and then discuss the results.

When classifying in GP we compute the distance from the test sample to all training samples and return the sum weighted by the covariance as defined in Equation (2). The covariance itself cannot leak the data: an inversion of the kernel is not possible. The attacker cannot recompute but only approximate the training data [43]. A single published sum is also unlikely to leak information [35].

On the other hand, taking GP as secure classifier as example, the output for all training points will be 1. In contrast, the output for all test points (assuming no duplicates) is  $< 1$ . Additionally, we have to distinguish between the mean and the variance in this setting: in contrast to the mean, a high variance always implies large distance from the training data.

We conclude that even though there are formal reasons to believe the GP does not leak membership, the attack has to be evaluated empirically.

### 7.1. Lengthscale and Membership Inference

**7.1.1. Setting.** We use the same datasets as in the previous experiments which we summarized in Table 2. Analogously to before, we implement our experiments in Python using GPy for the Gaussian Process approaches [20]. We use the previously found low and high lengthscales values. Our attacker has full access to training and test data and the corresponding output of GPC, either mean or variance, to train a model. As the output is a single, continuous variable, we train a decision tree, a random forest and an AdaBoost classifier. These classifiers can easily split a single feature in many small subsets, as needed in this case. We report the best achieved accuracy on a test set. As a baseline, we provide the random guess accuracy.

**7.1.2. Results.** We depict the results of our experiment in Figure 9. We observe that the variances increases the accuracy significantly. In particular when a GPC with short lengthscales trained on MNIST or SVHN is targeted, we observe accuracies of 100%. For the security datasets, the

increase is significant, but accuracy around  $< 85\%$  for the long and around 95% of the short lengthscales.

Concerning the mean, we observe that on a short lengthscales, we can improve accuracy significantly for the Malware and MNIST data. There are however few cases where the accuracy is significantly above random guess for a long lengthscales. The datasets affected are SVHN, and the two Malware datasets. Yet, the increase to compared to random guess is  $< 10\%$ .

The datasets where accuracy is slightly higher than random guess for a long lengthscales are also the datasets with the largest number of features. Since we train on small subsets of the training data, we retrained GPC with more data, up to 8.000 samples. We did however not find any consistent change in attack accuracy.

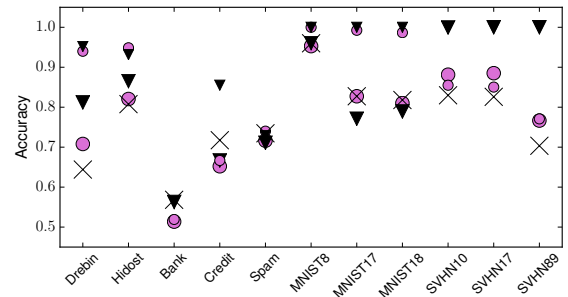


Figure 9. Lengthscale and membership inference on GPC. Circles represent accuracy of classifiers trained on mean. When training on variance, we depict triangles. Bigger symbols denote a long lengthscales of targeted GPC, small symbols a short. Random Guess Accuracy is denoted by x).

### 7.2. Conclusion on GP and Membership Inference

We reasoned that the mean of GP is unlikely to leak information on the training data used for a GP, and could empirically validate this when a long lengthscales is used. For a short lengthscales or the predictive variance, we observe that information about membership in training can be deduced. A short lengthscales might be related to over-fitting, or non-confident prediction, as also visible in the last section on poisoning. This aligns with previous work on this topic on other non-linear models [56].

## 8. Improving GP's Security

A problem increasing the vulnerability of ML is that there is few transparency. When arguing for a defense using high confidence [22], then this is still an abstract concept for some concrete data (although mathematically well defined). We want to propose a rethinking in this area, and propose a more transparent classification scheme. We call this classifier ParGP, due to a *parametrization*. Each parameter has a concrete interpretation (how many points are used in classification? How many of them agree?), based on a learned distance. We first introduce the scheme and its functionality and then relate it to other classifiers. In the next step, we evaluate it on benign and adversarial data.

## 8.1. ParGP's Classification Scheme

Before we introduce our own scheme, let us review the predictive mean of GP Regression given a test point  $x'$ .

$$\mu = \sigma \left( \sum_i \epsilon'(x', x_i) * K_i^{-1} * y_i \right), \quad (16)$$

where we sum over the weighted similarities of all training points. We now introduce the following parameters

- $l$  cutoff value or lengthscale.
- $v$  number of data points used for voting.
- $m$  minimal number of data points supporting vote.
- $r$  threshold needed for vote to be successful.

and replace the link function and the sum by a voting scheme. As a first step, we order the training points by distance to the corresponding test point. We then consider the first  $v$ . As we want the user to have more control about rejection, parameter  $m$  specifies how many points of  $v$  need to be non-zero at least.

We further introduce a threshold,  $r \in [0.5, 1.0]$ . This value defines how large the fraction of supporting samples of one class needs to be for the point to be classified. Setting  $r$  to 0.75, for example, means that a test point needs to be surrounded by  $0.75n$  ( $m \leq n \leq v$ ) points of the same class with a distance  $> 0$ . Given  $v$  neighbors, of which at least  $m$  are nonzero (otherwise we reject), we formalize

$$f(x') = \begin{cases} 1 & \text{iff } \sum_i^v (y_k = 1) > rk \\ -1 & \text{iff } \sum_i^v (y_k = -1) > rk \\ \text{reject} & \text{otherwise} \end{cases}$$

where we are able to report additionally to the output class why classification was not possible or the sample was rejected (for example,  $m$  was not met, or  $r$  not reached, etc). This further enhances transparency.

**Relation to Other Classifiers.** To give a better understanding of our technique, we express other classification strategies in terms of parameters of our method. We start deriving the original GP. Our technique implicitly uses weights equal to one — choosing them as  $K_{tr}^{-1}$ , setting  $v$  to the size of the training set,  $r = 0.5$ ,  $m = 0$  and finally using a link function, we obtain the original GPC.

Further, setting  $r = 0.5$ ,  $m = 0$ , this classifier is equivalent to a k-nearest neighbor classifier. In the context of covariance function  $k$ , however, we renamed  $k$  to  $v$  here. By choosing  $l$  appropriately and allowing rejection, we obtain a variant of the secure classifier as introduced in Equation (9).

## 8.2. Evaluation of ParGP

We evaluate our new classification scheme in practice on benign and malicious data. First, we briefly introduce a setting and consider a toy dataset to show how the parameters interact.

**8.2.1. Setting.** We use the same datasets as in the previous experiments, which we summarized in Table 2. Additionally, we employ the two moons dataset in two dimensions for visualization. For the experiments, we compute accuracy on benign data and how much of the benign data is rejected given a specific criterion. We implement our experiments in Python using GPy for the Gaussian Process part [20]. We reuse the adversarial data computed in Section 5.3.

**8.2.2. ParGP on a Toy Dataset.** To understand the introduced classification scheme for GP, we will first experiment with a toy dataset. to this end, we plot the output for different parameter settings on the two moons dataset.

We show the results in Figure 10. As a comparison, Figure 10a contains the dataset and the continuous classification function of an unmodified GPC. We show three different plots, where we observe that the lengthscale is best chosen smaller than in the original case. We can specify a small number of  $v$ , set a high threshold  $r$  and obtain thereby a classifier with a margin (as in Figure 10d compared to no margin in Figure 10c). In general,  $m$  is a parameter to control how far away from the data we classify. Using all data points in a voting system without weights, as done here leads to counterintuitive results, as shown in Figure 10b.

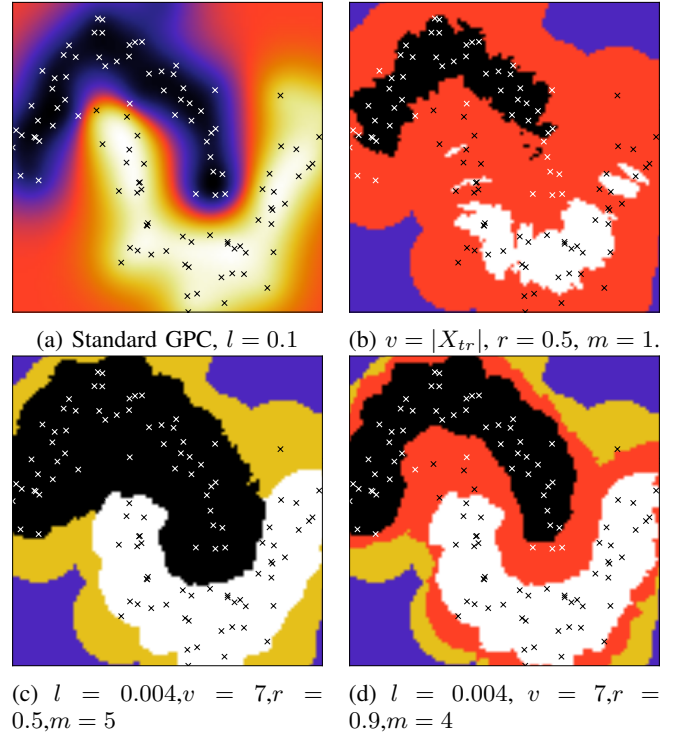


Figure 10. Influence of different parameter choices in ParGP on the two moons dataset. Black and White classify. Purple denotes that the mean is zero (similarity abates,  $l$ ), brown that the data does not back up the decision ( $m$  not met). Red denotes that decision was not backed up by enough points ( $r$ ).

**8.2.3. ParGP in Practice.** Given the previous visualization, we apply ParGP to real world data. We evaluate a range

of different values for  $v, r$ , and  $m$  as a proof of concept. In practice, these values have to be chosen specifically for a task. As we observed a much smaller lengthscale to be necessary, we vary the lengthscale between 1% and 10% of the original, best value. Generally, 10% of original works good and is used in the plots (as indicated). We further use a range of values for  $v$ , namely 1, 10, 25 and 50. For  $r$  we pick 0.5 (majority vote), 0.75 (three fourths of data voting for one class) and 0.9 (90% voting for the same class). We also vary  $m$ , where it is either 1 (e.g., one point) or 0.2, 0.4, 0.6, 0.8, the latter in percent of  $v$ . We either vary  $m$  (then  $r = 0.5$ ) or  $r$  (then  $m = 1$ ). To give an example,  $v = 10$  and  $m = 0.8$  means that of  $v$  nearest neighbors, 8 need a similarity which is nonzero. We varied  $m$ , so  $r = 0.5$ : 5 points have to agree on classification for an output that is not reject.

We plot the accuracy on benign test data and the percentage of rejected points given the criterion that is evaluated. Hence, accuracy and rejected percentage do not necessary sum up to one: misclassification or rejection due to other criteria lower the value as well. One criterion that is never excluded is rejection when all distances are zero.

We present our results in Figure 11. For benign data, there is generally no rejection due to  $m$ . In contrast, there is high rejection due to  $r$  on for example Credit, Spam and SVHN subtasks. Intuitively, more data is rejected when  $r$  is larger. We observe in all cases without high rejection percentage that the accuracy is higher than a random guess on the dataset.

**8.2.4. ParGP and Test Time Attacks.** We now evaluate the vulnerability of ParGP in the presence of malicious data. We reuse the adversarial examples computed in Section 5.3 for this purpose. An overview of the used datasets and configurations is given in Table 4. After an initial evaluation, only few settings remain where the maximum decrease in accuracy is not more than 6%. We first discuss the accuracy on adversarial data, and afterwards which criteria rejected the manipulated data.

We plot the accuracy on adversarial examples in Figure 12. We observe that ParGP on the bank dataset is still vulnerable. This is the setting with lowest  $r$ , however. For Hidost, all accuracies are higher than 99.8%. For MNIST91, all accuracies are higher than 99%. There is one exception for MNIST91, which is the attack crafted on DNN using  $\epsilon = 0.4$  with only 97.8%. A notable exception for both MNIST91 and Hidost are the linear SVM attacks, which are both much worse with 55% and 93%.

To obtain a baseline, we compare ParGP to the best result of GP with short and long lengthscale and with and without rejection option. We always take the highest accuracy from any of the four as our baseline. On average, ParGP outperforms the baseline. In particular on optimized attacks such as  $L_2$  and Jacobian based methods, ParGP achieves good results.

Concerning rejection, analogous to benign data, there are no rejections due to  $m$ . We observed rejection due  $\mu = 0$  only in 6% of the cases and only on MNIST91. In contrast, there are rejections due to  $r$  in all evaluated settings. The

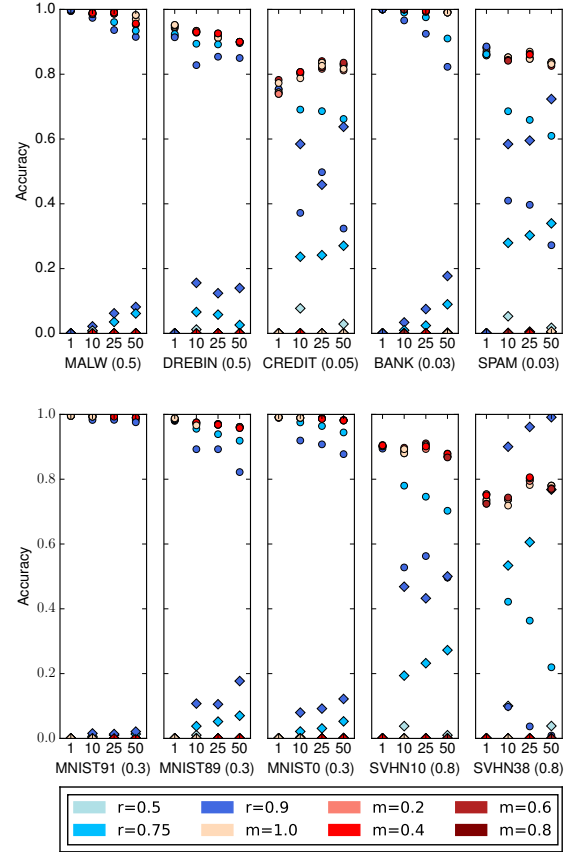


Figure 11. ParGP with different parameters on different datasets. Dots are accuracy (on  $x$ -axis, same for all plots), diamonds rejection due to tested criterion. The value below each plot denotes  $v$ , where each plot is assigned to one lengthscale/dataset combination. We further plot  $r$  (blue) and  $m$  (red) (in percent of  $v$ ), where in both cases a darker color indicates a higher threshold.

TABLE 4. PARGP PARAMETER AND REJECTIONS.

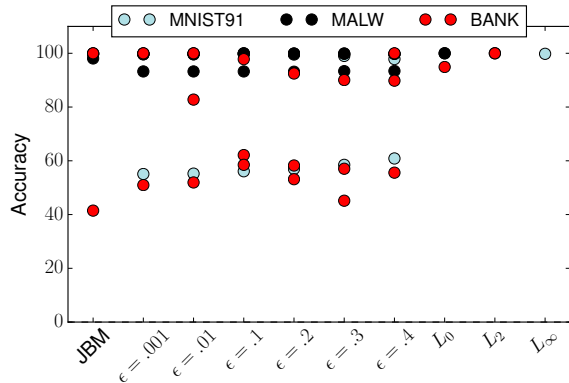
| Data    | parameters |      |     | Acc.  | rejection (malicious) |      |           |
|---------|------------|------|-----|-------|-----------------------|------|-----------|
|         | $v$        | $r$  | $m$ |       | $\mu = 0$             | $r$  | % due $r$ |
| Hidost  | 10         | 0.9  | 0.8 | 96.5% | 0%                    | 100% | 6.4%      |
| Bank    | 25         | 0.75 | 0.8 | 96.8% | 0%                    | 100% | 8.6%      |
| MNIST91 | 50         | 0.9  | 0.8 | 93.4% | 6%                    | 100% | 16.8%     |

percentage of this samples is with 6% to 17% however quite low.

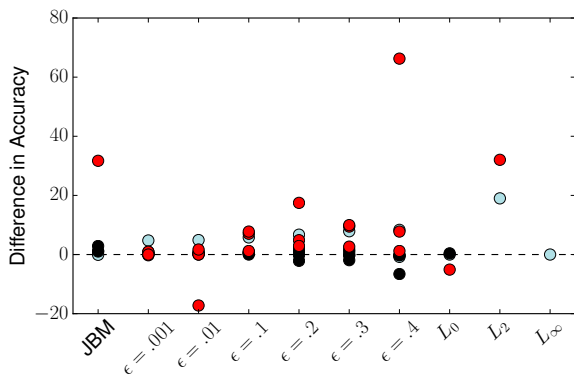
### 8.3. Conclusion on ParGP

We conclude that a parametrized classification scheme can be applied in practice, albeit at a reduced accuracy. In two of three settings, we observed promising results on adversarial data. Yet, the evaluation also show how important it is to use diverse attacks in evaluation: The accuracy on adversarial examples computed on a linear SVM was improved, but ParGP is still vulnerable. Yet, we consider





(a) Percent of correctly classified or rejected adversarial data.



(b) Compared to best GPC - positive number is improve in percent accuracy.

Figure 12. ParGPC classification on adversarial examples.

this approach as a first step, adapting GP’s optimization to the voting to achieve better results is left as future work. We did not evaluate on the poisoning attacks, as they can be countered straight forwardly by choosing high  $v$  and  $r$ .

## 9. Related Work

We first review adversarial learning in the Bayesian context, and then turn to other formal methods in the context of adversarial learning. Afterwards, we review regularization and finally mitigations in adversarial ML that are related.

**Bayesian Learning and Adversarial Learning.** Other works done by Bradshaw et al. [9], and Rawat et al. [40] investigate adversarial learning in the context of the Bayesian framework. They do not concern GP in particular, however. Grosse et al. [22] propose test time attacks on GP and investigate their impact on uncertainty. All of them, however, take an empirical approach and further only investigate test time attacks.

**Formal Approaches to Adversarial Machine Learning.** Fawzi et al. [18] show general vulnerability for all classifiers. Similarly, Wang et al. [53] show the vulnerability

TABLE 5. SUMMARIZED RESULTS.

| Attack               | optimal curvature | comments                          |
|----------------------|-------------------|-----------------------------------|
| Test time            | none              | improve with rejection (steep)    |
| Training time        | rather flat       |                                   |
| Membership inference | flat              | only releasing mean, not variance |

for the k-nearest-neighbor classifier, where they define robustness given a  $\rho$ -ball, analogous to our approach. Yet, their approach works in the infinite sample limit, and they propose deletion of points as countermeasure. Both approaches contrast to the extension of our analysis to poisoning and membership inference, and further to our effort to more transparent classification.

Further Tanay and Griffin [14] propose as well a radius classifier, however in context of SVM. They focus on decision plane classification without rejection option. In contrast, we work on non-linear methods without decision planes.

**Regularization, Vulnerability, and Mitigations.** Russu et al. [41] show a relationship between the gradient of a linear model and its vulnerability. Previous defenses for DNN can be linked to regularization, as for example in Lyu et al. [29]. In contrast, we find evidence that in non-linear methods, regularization will change, not solve the problem.

Another line of work in DNN has a strong relation to the secure classifier proposed in Equation (9). Several forms of adversarial training, as proposed by Madry et al. [30], Sinha et al. [45] and Wong et al. [55] aim directly at training the network to output the same class in a  $\rho$ -ball around each training point. Yet these approaches do not consider a reject option, which has however been done empirically by Melis et al. [32]. For example Bendale and Boulton [4] write about open set recognition in general. We however connect both ideas, rejection and  $\rho$ -balls, in our work.

Finally, Papernot and McDaniel [38] connect explainability and adversarial learning for test time attacks. We work along those lines with ParGP, allowing however parameters on *how classification is computed* instead of *explaining* a given classification.

## 10. Conclusion

We investigated several attack vectors on classification. Given a naive secure classifier at test time expressed as a GP, we formally showed that learning is opposed to static security guarantees. We further identified the curvature of the classifier as a factor in robustness to attacks, and used GP as a framework to study the influence of curvature on a range of datasets and attack vectors.

In the case of test time attacks, curvature only changes the kind of attack that needs to be applied to succeed. This emphasizes a diverse collection of attacks when evaluating a defense. For training time attacks, we observe a slight advantage when using a flat decision function. For membership inference, the improvement over random guess with flat curvature is less than 10%. With a steep function,

eight of eleven attacks achieve more than 90% accuracy. We summarize our findings in Table 5.

As a consequence of the previous results, we define a voting scheme. It allows fine grained control on how many points support a test point and how large the agreement on one class is among those points. This defends poisoning, as potentially many points have to be introduced. The scheme also shows promising results on adversarial examples: It enables us to define a setting where only very high confidence samples are classified.

## Acknowledgment

This work was supported by the German Federal Ministry of Education and Research (BMBF) through funding for the Center for IT-Security, Privacy and Accountability (CISPA) (FKZ: 16KIS0753). This work has further been supported by the Engineering and Physical Research Council (EPSRC) Research Project EP/N014162/1.

## References

- [1] M. Abadi, A. Agarwal, P. Barham, E. Brevdo, Z. Chen, C. Citro, G. S. Corrado, A. Davis, J. Dean, M. Devin, S. Ghemawat, I. Goodfellow, A. Harp, G. Irving, M. Isard, Y. Jia, R. Jozefowicz, L. Kaiser, M. Kudlur, J. Levenberg, D. Mané, R. Monga, S. Moore, D. Murray, C. Olah, M. Schuster, J. Shlens, B. Steiner, I. Sutskever, K. Talwar, P. Tucker, V. Vanhoucke, V. Vasudevan, F. Viégas, O. Vinyals, P. Warden, M. Wattenberg, M. Wicke, Y. Yu, and X. Zheng. TensorFlow: Large-scale machine learning on heterogeneous systems, 2015. Software available from tensorflow.org.
- [2] D. Arp, M. Spreitzenbarth, M. Hubner, H. Gascon, and K. Rieck. DREBIN: Effective and Explainable Detection of Android Malware in Your Pocket. In *Proceedings of the 2014 Network and Distributed System Security Symposium (NDSS)*, 2014.
- [3] A. Athalye, N. Carlini, and D. Wagner. Obfuscated Gradients Give a False Sense of Security: Circumventing Defenses to Adversarial Examples. *ArXiv e-prints*, Feb. 2018.
- [4] A. Bendale and T. E. Boulton. Towards open set deep networks. In *2016 IEEE Conference on Computer Vision and Pattern Recognition, CVPR 2016, Las Vegas, NV, USA, June 27-30, 2016*, pages 1563–1572, 2016.
- [5] B. Biggio, I. Corona, D. Maiorca, B. Nelson, N. Srndic, P. Laskov, G. Giacinto, and F. Roli. Evasion attacks against machine learning at test time. In *Machine Learning and Knowledge Discovery in Databases - European Conference, ECML PKDD 2013, Prague, Czech Republic, September 23-27, 2013, Proceedings, Part III*, pages 387–402, 2013.
- [6] B. Biggio, G. Fumera, F. Roli, and L. Didaci. Poisoning adaptive biometric systems. In *Structural, Syntactic, and Statistical Pattern Recognition - Joint IAPR International Workshop, SSPR&SPR 2012, Hiroshima, Japan, November 7-9, 2012. Proceedings*, pages 417–425, 2012.
- [7] B. Biggio, B. Nelson, and P. Laskov. Poisoning attacks against support vector machines. In *Proceedings of the 29th International Conference on Machine Learning, ICML 2012, Edinburgh, Scotland, UK, June 26 - July 1, 2012*, 2012.
- [8] P. Blanchard, E. Mahdi El Mhamdi, R. Guerraoui, and J. Stainer. Byzantine-Tolerant Machine Learning. *ArXiv e-prints*, Mar. 2017.
- [9] J. Bradshaw, A. G. d. G. Matthews, and Z. Ghahramani. Adversarial Examples, Uncertainty, and Transfer Testing Robustness in Gaussian Process Hybrid Deep Networks. *ArXiv e-prints*, July 2017.
- [10] M. Brückner and T. Scheffer. Stackelberg games for adversarial prediction problems. In *Proceedings of the 17th ACM SIGKDD International Conference on Knowledge Discovery and Data Mining, San Diego, CA, USA, August 21-24, 2011*, pages 547–555, 2011.
- [11] N. Carlini and D. Wagner. Towards evaluating the robustness of neural networks. *CoRR*, abs/1608.04644, 2016.
- [12] N. Carlini and D. A. Wagner. Adversarial examples are not easily detected: Bypassing ten detection methods. *CoRR*, abs/1705.07263, 2017.
- [13] M. Cisse, Y. Adi, N. Neverova, and J. Keshet. Houdini: Fooling Deep Structured Prediction Models. *ArXiv e-prints*, July 2017.
- [14] T. M. Cover and J. A. Thomas. *Elements of information theory* (2. ed.). Wiley, 2006.
- [15] G. Cretu, A. Stavrou, M. Locasto, S. Stolfo, and A. Keromytis. Casting out demons: Sanitizing training data for anomaly sensors. In *Security and Privacy, 2008. SP 2008. IEEE Symposium on*, pages 81–95, may. 2008.
- [16] A. Demontis, M. Melis, B. Biggio, D. Maiorca, D. Arp, K. Rieck, I. Corona, G. Giacinto, and F. Roli. Yes, machine learning can be more secure! A case study on android malware detection. *CoRR*, abs/1704.08996, 2017.
- [17] I. Evtimov, K. Eykholt, E. Fernandes, T. Kohno, B. Li, A. Prakash, A. Rahmati, and D. Song. Robust Physical-World Attacks on Machine Learning Models. *ArXiv e-prints*, July 2017.
- [18] A. Fawzi, H. Fawzi, and O. Fawzi. Adversarial vulnerability for any classifier. *ArXiv e-prints*, Feb. 2018.
- [19] I. J. Goodfellow, N. Papernot, and P. D. McDaniel. cleverhans v0.1: an adversarial machine learning library. *CoRR*, abs/1610.00768, 2016.
- [20] GPy. GPy: A gaussian process framework in python. <http://github.com/SheffieldML/GPy>, since 2012.
- [21] K. Grosse, N. Papernot, P. Manoharan, M. Backes, and P. D. McDaniel. Adversarial examples for malware detection. In *Computer Security - ESORICS 2017 - 22nd European Symposium on Research in Computer Security, Oslo, Norway, September 11-15, 2017, Proceedings, Part II*, pages 62–79, 2017.
- [22] K. Grosse, D. Pfaff, M. T. Smith, and M. Backes. How Wrong Am I? - Studying Adversarial Examples and their Impact on Uncertainty in Gaussian Process Machine Learning Models. *ArXiv e-prints*, Nov. 2017.
- [23] S. Gu and L. Rigazio. Towards deep neural network architectures robust to adversarial examples. *CoRR*, abs/1412.5068, 2014.
- [24] J. Hayes, L. Melis, G. Danezis, and E. De Cristofaro. LOGAN: Evaluating Privacy Leakage of Generative Models Using Generative Adversarial Networks. *ArXiv e-prints*, May 2017.
- [25] M. Hein and M. Andriushchenko. Formal Guarantees on the Robustness of a Classifier against Adversarial Manipulation. *ArXiv e-prints*, May 2017.
- [26] R. Laishram and V. V. Phoha. Curie: A method for protecting SVM classifier from poisoning attack. *CoRR*, abs/1606.01584, 2016.
- [27] Y. LeCun, L. Bottou, Y. Bengio, and P. Haffner. Gradient-based learning applied to document recognition. *Proceedings of the IEEE*, 86(11):2278–2324, November 1998.
- [28] M. Lichman. UCI machine learning repository, 2013.
- [29] C. Lyu, K. Huang, and H. Liang. A unified gradient regularization family for adversarial examples. In *2015 IEEE International Conference on Data Mining, ICDM 2015, Atlantic City, NJ, USA, November 14-17, 2015*, pages 301–309, 2015.
- [30] A. Madry, A. Makelov, L. Schmidt, D. Tsipras, and A. Vladu. Towards Deep Learning Models Resistant to Adversarial Attacks. *ArXiv e-prints*, June 2017.



- [31] S. Mei and X. Zhu. Using machine teaching to identify optimal training-set attacks on machine learners. In *Proceedings of the Twenty-Ninth AAAI Conference on Artificial Intelligence, January 25-30, 2015, Austin, Texas, USA.*, pages 2871–2877, 2015.
- [32] M. Melis, A. Demontis, B. Biggio, G. Brown, G. Fumera, and F. Roli. Is deep learning safe for robot vision? adversarial examples against the icub humanoid. In *2017 IEEE International Conference on Computer Vision Workshops, ICCV Workshops 2017, Venice, Italy, October 22-29, 2017*, pages 751–759, 2017.
- [33] S. Mika, G. Ratsch, J. Weston, B. Scholkopf, and K. R. Mullers. Fisher discriminant analysis with kernels. In *Neural Networks for Signal Processing IX: Proceedings of the 1999 IEEE Signal Processing Society Workshop (Cat. No.98TH8468)*, pages 41–48, Aug 1999.
- [34] L. Muñoz-González, B. Biggio, A. Demontis, A. Paudice, V. Wongrassamee, E. C. Lupu, and F. Roli. Towards poisoning of deep learning algorithms with back-gradient optimization. In *AISeC@CCS*, pages 27–38. ACM, 2017.
- [35] S. U. Nabar, K. Kenthapadi, N. Mishra, and R. Motwani. A survey of query auditing techniques for data privacy. In *Privacy-Preserving Data Mining - Models and Algorithms*, pages 415–431. 2008.
- [36] Y. Netzer, T. Wang, A. Coates, A. Bissacco, B. Wu, and A. Y. Ng. Reading digits in natural images with unsupervised feature learning. In *NIPS Workshop on Deep Learning and Unsupervised Feature Learning 2011*, 2011.
- [37] N. Papernot, P. McDaniel, S. Jha, M. Fredrikson, Z. B. Celik, and A. Swami. The Limitations of Deep Learning in Adversarial Settings. In *Proceedings of the 1st IEEE European Symposium in Security and Privacy (EuroS&P)*, 2016.
- [38] N. Papernot and P. D. McDaniel. Deep k-nearest neighbors: Towards confident, interpretable and robust deep learning. *CoRR*, abs/1803.04765, 2018.
- [39] C. E. Rasmussen and C. K. I. Williams. *Gaussian processes for machine learning*. Adaptive computation and machine learning. MIT Press, 2006.
- [40] A. Rawat, M. Wistuba, and M.-I. Nicolae. Adversarial Phenomenon in the Eyes of Bayesian Deep Learning. *ArXiv e-prints*, Nov. 2017.
- [41] P. Russu, A. Demontis, B. Biggio, G. Fumera, and F. Roli. Secure kernel machines against evasion attacks. In *AISeC@CCS*, pages 59–69. ACM, 2016.
- [42] W. J. Scheirer, L. P. Jain, and T. E. Boult. Probability models for open set recognition. *IEEE Trans. Pattern Anal. Mach. Intell.*, 36(11):2317–2324, 2014.
- [43] B. Schölkopf, S. Mika, C. J. C. Burges, P. Knirsch, K. Müller, G. Rätsch, and A. J. Smola. Input space versus feature space in kernel-based methods. *IEEE Trans. Neural Networks*, 10(5):1000–1017, 1999.
- [44] R. Shokri, M. Stronati, and V. Shmatikov. Membership Inference Attacks against Machine Learning Models. *ArXiv e-prints*, Oct. 2016.
- [45] A. Sinha, H. Namkoong, and J. Duchi. Certifiable distributional robustness with principled adversarial training. *arXiv preprint arXiv:1710.10571*, 2017.
- [46] C. Sitawarin, A. Nitin Bhagoji, A. Mosenia, M. Chiang, and P. Mittal. DARTS: Deceiving Autonomous Cars with Toxic Signs. *ArXiv e-prints*, Feb. 2018.
- [47] M. T. Smith, M. Zwiessle, and N. D. Lawrence. Differentially private gaussian processes. *arXiv preprint arXiv:1606.00720*, 2016.
- [48] N. Šrndić and P. Laskov. Practical evasion of a learning-based classifier: A case study. In *2014 IEEE Symposium on Security and Privacy, SP 2014, Berkeley, CA, USA, May 18-21, 2014*, pages 197–211, 2014.
- [49] N. Šrndić and P. Laskov. Hidost: a static machine-learning-based detector of malicious files. *EURASIP Journal on Information Security*, 2016(1):22, Sep 2016.
- [50] J. Steinhardt, P. W. Koh, and P. Liang. Certified Defenses for Data Poisoning Attacks. *ArXiv e-prints*, June 2017.
- [51] R. Stevens, O. Suci, A. Ruef, S. Hong, M. Hicks, and T. Dumitraş. Summoning Demons: The Pursuit of Exploitable Bugs in Machine Learning. *ArXiv e-prints*, Jan. 2017.
- [52] C. Szegedy, W. Zaremba, I. Sutskever, J. Bruna, D. Erhan, I. J. Goodfellow, and R. Fergus. Intriguing properties of neural networks. *CoRR*, abs/1312.6199, 2013.
- [53] Y. Wang, S. Jha, and K. Chaudhuri. Analyzing the robustness of nearest neighbors to adversarial examples. *CoRR*, abs/1706.03922, 2017.
- [54] Z. Wang, A. C. Bovik, H. R. Sheikh, and E. P. Simoncelli. Image quality assessment: from error visibility to structural similarity. *IEEE Transactions on Image Processing*, 13(4):600–612, April 2004.
- [55] E. Wong and J. Zico Kolter. Provable defenses against adversarial examples via the convex outer adversarial polytope. *ArXiv e-prints*, Nov. 2017.
- [56] S. Yeom, M. Fredrikson, and S. Jha. The Unintended Consequences of Overfitting: Training Data Inference Attacks. *ArXiv e-prints*, Sept. 2017.